

Estimating the Residual Axial Load Capacity of Flexure-dominated Reinforced Concrete Bridge Columns



**Morgan State University
The Pennsylvania State University
University of Maryland
University of Virginia
Virginia Polytechnic Institute & State University
West Virginia University**

**The Pennsylvania State University
The Thomas D. Larson Pennsylvania Transportation Institute
Transportation Research Building ❖ University Park, PA 16802-4710
Phone: 814-865-1891 ❖ Fax: 814-863-3707
www.mautc.psu.edu**

1. Report No. PSU-2013-03	2. Government Accession No.	3. Recipient's Catalog No.	
4. Title and Subtitle Estimating the Residual Axial Load Capacity of Flexure-dominated Reinforced Concrete Bridge Columns		5. Report Date 8/11/2014	
		6. Performing Organization Code	
7. Author(s) Gordon Warn and Mehmet Unal		8. Performing Organization Report No. LTI 2015-05	
9. Performing Organization Name and Address The Pennsylvania State University Larson Transportation Institute 201 Transportation Research Building University Park, PA 16802		10. Work Unit No. (TRAIS)	
		11. Contract or Grant No. DTRT12-G-UTC03	
12. Sponsoring Agency Name and Address US Department of Transportation Research & Innovative Technology Administration UTC Program, RDT-30 1200 New Jersey Ave., SE Washington, DC 20590		13. Type of Report and Period Covered Final 01/01/2013 – 06/30/14	
		14. Sponsoring Agency Code	
15. Supplementary Notes COTR: Dawn Tucker-Thomas, M.S., J.D., Senior Transportation Specialist			
16. Abstract Extreme events such as earthquakes have the potential to damage hundreds, if not thousands, of bridges on a transportation network. Following an earthquake, the damaged bridges are inspected by engineers sequentially to decide whether or not to close the bridges to traffic. These inspections are generally slow and resource intensive, potentially leading to traffic disruption on the network for a long period of time. A recent experimental study on reinforced concrete bridge columns demonstrated that the bridge columns designed according to modern design specifications and standards, e.g. Caltrans Seismic Design Criteria (SDC), exhibited approximately 80% of their original axial capacity after being subjected to cyclic lateral loading up to 4% drift. Thus, bridge columns designed following modern design requirements might possess significant residual axial load capacity even with the presence of moderate to extensive damage. A practical and efficient method for estimating the residual capacity of seismically damaged bridges would expedite bridge inspection and decision making regarding closure by allowing transportation agency officials to use the estimates to triage the on-site, visual inspection that would in turn minimize disruption to the transportation network by preventing overly conservative and unnecessary bridge closures. The objective of this study was to develop a practical mechanics-based method for accurately and efficiently estimating the residual axial load capacity of bridge columns given a level of seismic demand, measured by basic sensors instrumented on the bridge. The practical mechanics-based method for estimating the residual capacity of bridge columns was validated using experimental data from the axial testing of damaged column specimens designed according to Caltrans SDC. From the results of the validation study, the practical method was demonstrated to estimate the residual axial load capacity of bridge columns within approximately 3% accuracy when compared to experimental study results.			
17. Key Words Reinforced concrete bridge columns, seismic damage, residual axial load capacity, mechanics-based model, flexure-dominated		18. Distribution Statement No restrictions. This document is available from the National Technical Information Service, Springfield, VA 22161	
19. Security Classif. (of this report) Unclassified	20. Security Classif. (of this page) Unclassified	21. No. of Pages 35	22. Price

DISCLAIMER

The contents of this report reflect the views of the authors, who are responsible for the facts and the accuracy of the information presented herein. This document is disseminated under the sponsorship of the U.S. Department of Transportation's University Transportation Centers Program, in the interest of information exchange. The U.S. Government assumes no liability for the contents or use thereof.

Table of Contents

1	Introduction	1
2	Objective of research	2
3	Scope	2
4	Significance	3
5	Background.....	3
6	Finite element modeling	7
7	Practical method	12
7.1	Determination of the uncrushed area of the column	13
7.2	Residual axial capacity of concrete region of column	18
7.3	Residual axial load capacity of reinforcing steel bars.....	19
8	Validation of the model	21
9	Sensitivity analysis	25
10	Summary and conclusions	28
11	References.....	29

List of Figures

Figure 1. Degradation of axial load carrying capacity of laterally damaged columns (Terzic and Stojadinovic 2010).....	7
Figure 2. Finite element modeling details: (a) Prototype bridge column; (b) Fiber-element model of the column; (c) Fiber configuration of a cross section	8
Figure 3. Geometry and reinforcement details of specimens (Terzic and Stojadinovic, 2010): (a) elevation profile; (b) cross section (A-A)	9
Figure 4. Lateral force-displacement response for specimen Base 45: (a) in X direction; (b) in Y direction.....	10
Figure 5. Axial force-displacement relationship for finite element modeling and experimental results for specimens: (a) Base 0; (b) Base 15; (c) Base 30; (d) Base 45	11
Figure 6. Flowchart of the practical method.....	12
Figure 7. Equilibrium and compatibility diagram at the maximum displacement	14
Figure 8. Inelastic deformation of a bridge column (adapted from Priestley et al. 1996)	16
Figure 9. Force equilibrium on the column	16
Figure 10. Material models used in the practical method: (a) concrete; (b) reinforcing steel	18
Figure 11. Plastic strength of a reinforcing bar.....	21
Figure 12. Comparison of residual axial load capacity estimation to experimental results	24
Figure 13. Relative error in residual axial capacity estimation for each specimen	24
Figure 14. Sensitivity indices for each specimen.....	27

List of Tables

Table 1. Definitions of damage states by HAZUS (FEMA, 2003).....	5
Table 2. Ductility limits for each damage states.....	6
Table 3. Material properties of specimens	9
Table 4. Lateral loading information, observed damage and residual axial load capacity of specimens	22
Table 5. The input parameters for the mechanistic model.....	23
Table 6. Parameters and parameter ranges considered in the sensitivity analysis.....	26

1 Introduction

Bridges are vulnerable links of transportation networks. An extreme event, such as an earthquake, can damage hundreds of bridges in a given region. Following an earthquake, department of transportation (DOT) officials visit and visually inspect (INDOT, 2000) each bridge to decide whether the bridge should remain closed, be reopened to emergency vehicles only, or be reopened to all traffic. However, these visual inspections require tremendous resources, both physical and human, and are sequential in nature, requiring long periods of time to assess the integrity of the entire bridge stock in a given region. During the inspection period, closures disrupt traffic operations on the roadway network, reducing the mobility of goods and services that translates into potentially significant economic and societal losses. During visual inspections, indicators of damage such as the extent of cracking, length and width of cracks, loss of concrete cover, and buckling of reinforcing bars are noted. Based on these indicators and largely engineering judgment a decision is made whether the bridge should remain closed or be reopened, using a conservative approach in order to maintain a high level of public safety. However, if the approach is overly conservative, many bridges that are structurally safe will remain closed, severely disrupting operations on the roadway network. Rapid, yet rigorous estimation of the residual capacity of bridges subjected to earthquake ground shaking could allow transportation agency officials to expedite decision-making and the inspection process following an event by using the residual capacity estimates to triage visual bridge inspection. Furthermore, bridges with a significant percentage of residual capacity, e.g. greater than 90% of the undamaged, could be reopened in lieu of a detailed visual inspection, thereby reducing the economic and societal impacts of earthquake events.

Past research that examined the post-earthquake capacity of bridge columns, which are the most vulnerable elements of bridges (Berry and Eberhard 2004), demonstrated that reinforced concrete bridge columns designed following modern design specifications, such as Caltrans Seismic Design Criteria (SDC) (2006), retain a significant percentage of their undamaged vertical load-carrying capacity even after several cycles of lateral loading (Mackie and Stojadinovic 2005, Terzic and Stojadinovic 2010). For example, Terzic and Stojadinovic (2010) experimentally demonstrated that a $\frac{1}{4}$ -scale bridge column subjected to 4% drift retained 80% of its undamaged vertical load-carrying capacity. A number of studies (Tasai 1999, Tasai 2000, Kato and Ohnishi

2001, Elwood and Moehle 2005) have investigated vertical load capacity degradation of reinforced concrete columns. However, these studies developed analytical models on rectangular building columns having mostly shear degradation during seismic excitation. For columns possessing dominant flexural behavior, a highly detailed modeling using finite element methods has been shown to simulate the residual capacity with high fidelity, but these models are resource intensive to develop and computationally intensive to run. However, there has not yet been an attempt to develop a practical and efficient method for accurately and efficiently estimating the residual capacity of flexure-dominated bridge columns so that the permissible traffic load can be determined.

2 Objective of Research

The aim of this study was to develop a practical, mechanics-based method for estimating the residual axial load capacity of modern, flexure-dominated bridge columns given structural demands. It was assumed the structural demands can be obtained either through instrumentation installed on the bridge or through simulation. Finite element modeling of experimentally tested bridge columns was conducted to verify the adequacy of highly detailed structural analysis methods. Once the accuracy of existing, highly detailed structural analysis methods was established, a simplified, mechanics-based method was developed for estimating the residual vertical capacity of flexure-dominated reinforced concrete columns given a particular demand (e.g., drift ratio). The fidelity of the practical method was assessed using experimental data from Terzic and Stojadinovic (2010). Following validation of the practical method, a sensitivity analysis of the method was performed to understand the relative importance of the parameters on the estimation of residual axial capacity to determine whether further simplifications are possible.

3 Scope

In this study, the focus was on developing a practical method for estimating the residual axial load capacity of flexure-dominated, single-column bridge bents designed according to modern design requirements and specifications (Caltrans SDC 2006). Validation utilized the results of past experimental studies on single cantilever bridge columns performed by Terzic and Stojadinovic (2010). Estimating the residual axial load capacity of shear dominated columns

was also important, and there exist a number of scholarly studies (Tasai 1999, Tasai 2000, Kato and Ohnishi 2001, Elwood and Moehle 2005), but developing a practical model for shear dominated columns was outside the scope of the present study.

4 Significance

Following an earthquake, the residual traffic capacity of damaged bridges on the network needs to be estimated rapidly to reduce the economic impacts due to bridge closures. A practical method to accurately estimate the residual axial load capacity of bridge columns using mechanistic relationships, rather than using complex finite element modeling techniques, can facilitate a rapid post-event assessment of residual capacity and thus permissible traffic load. This practical method will allow Department of Transportation officials to triage visual bridge inspections, thus allowing for more efficient utilization of human and physical resources and reducing the likelihood of unnecessary bridge closures and thus traffic disruption. Furthermore, the practical and computationally efficient method developed in this study can be adopted by other researchers to provide a fundamental link between earthquake demand and permissible traffic flow for assessing the impact of regional hazards on transportation networks for disaster planning and loss estimation.

5 Background

The performance of reinforced concrete bridge columns during earthquakes has been investigated by a number of researchers over the past five decades (e.g., Munro et al. 1976, Kunnath et al. 1997, Lehman and Moehle 2000, Henry and Mahin 1999, and Moyer and Kowalsky 2001). The common objectives of these studies was to understand damage sustained (e.g., type and extent of cracking, reinforcement buckling, reinforcement fracture) for a given level of earthquake demand (e.g., drift ductility and rotation). Although many elements of the bridge are vulnerable to earthquake-induced damage, the bridge bent columns were the focus of these studies because failure of the columns can lead to complete collapse of the bridge (Berry and Eberhard 2004). By using the results of these experimental studies, analytical models on reinforced concrete bridge columns have been developed and new design recommendations have been proposed (e.g., Hachem et al. 2003, Berry and Eberhard 2004). Despite numerous experimental and analytical studies on the seismic performance of columns, only a few studies

(Tasai 1999, Tasai 2000, Kato and Ohnishi 2001, Elwood and Moehle 2005, Mackie and Stojadinovic 2005, Terzic and Stojadinovic 2010) have critically examined the post-earthquake or “residual” axial load capacity of reinforced concrete columns. The studies of Stojadinovic (2005, 2010) in particular have focused on assessing the permissible traffic load of damaged bridge columns through both experimental hybrid simulation and highly detailed finite element modeling.

Axial load capacity degradation of reinforced concrete columns has been studied analytically by a number of researchers (Tasai 1999, Tasai 2000, Kato and Ohnishi 2001, Elwood and Moehle 2005). However, these studies developed analytical models on rectangular building columns having mostly shear degradation during seismic excitation. Tasai (1999, 2000) proposed an analytical model to estimate the residual axial load capacity of building columns based on truss-arch mechanisms where the bond stresses and hoop stresses are used to compute truss and arch forces. It is assumed that the truss mechanism forms after the generation of dominant shear cracks. The need for the bond and hoop stresses at every loading instant makes it impractical to estimate residual axial load capacity of damaged reinforced concrete columns. Kato and Ohnishi (2001) developed an empirical model using 132 rectangular reinforced concrete column specimens to find the deflections at which the axial load capacity is lost. Elwood and Moehle (2005) used a shear-friction model to estimate the residual axial load capacity of reinforced concrete building columns that have experienced shear failure during earthquakes. The model takes into account the frictional forces on an idealized diagonal shear crack plane. The effective coefficient of shear friction at axial failure is estimated using the results of past experiments on column specimens. Although these past studies developed models to estimate residual axial load capacity of reinforced concrete columns, these models are not capable of estimating the residual axial capacity of flexure-dominated bridge columns because they are either based on shear crack mechanisms or use experimental data from rectangular building column specimens.

The study by Terzic and Stojadinovic (2010) in particular is one of the few studies that provides experimental data on the residual capacity of reinforced concrete bridge columns subjected to cyclic lateral loading via hybrid simulation techniques. In this experimental study, three bridge column specimens representing prototype highway overpass bridges designed according to modern design guidelines (Caltrans SDC 2006) were subjected to two-phase testing. The first

phase was bilateral quasi-static testing, where the specimens were displaced up to a pre-determined level of displacement ductility. The second phase was the axial compression of the laterally damaged specimens, which was applied until the specimens failed. One additional specimen was also tested only by axial compression to determine the undamaged capacity of column specimens. Each specimen was tested until it reached a ductility level that falls into one of the damage states, except for the collapse damage state, which are commonly used in performance-based earthquake engineering. Definitions of these damage states are described by HAZUS (FEMA 2003) and presented in Table 1. The most widely used quantitative definitions, based on the column ductility level and column drifts corresponding to each HAZUS damage state, are presented in Table 2.

Table 1. Definitions of damage states by HAZUS (FEMA, 2003)

<i>Damage States</i>	<i>Definitions</i>
None	No bridge damage.
Slight/Minor	Minor cracking and spalling to the abutment, cracks in shear keys at abutments, minor spalling and cracks at hinges, minor spalling at the column (damage requires no more than cosmetic repair), or minor cracking to the deck.
Moderate	Any column experiencing moderate (shear cracks) cracking and spalling (column structurally still sound), moderate movement of the abutment (<2 inches), extensive cracking and spalling of shear keys, any connection having cracked shear keys or bent bolts, keeper bar failure without unseating, rocker bearing failure or moderate settlement of the approach.
Extensive	Any column degrading without collapse, shear failure (column structurally unsafe), significant residual movement at connections, major settlement approach, vertical offset of the abutment, differential settlement at connections, shear key failure at abutments.
Complete	Any column collapsing and connection losing all bearing support, which may lead to imminent deck collapse, tilting of substructure due to foundation failure.

Table 2. Ductility limits for each damage states

<i>Damage State</i>	<i>Column Ductility (Choi et al. 2004)</i>	<i>Column Drift (Basoz and Mander 1999)</i>
None	$0 < \mu < 1$	$0 < \Delta/L < 0.01$
Slight/Minor	$1 < \mu < 2$	$0.01 < \Delta/L < 0.025$
Moderate	$2 < \mu < 4$	$0.025 < \Delta/L < 0.05$
Extensive	$4 < \mu < 7$	$0.05 < \Delta/L < 0.075$
Complete	$7 < \mu$	$0.075 < \Delta/L$

The results of the experimental study by Terzic and Stojadinovic (2010) demonstrated that the residual traffic capacity of bridge columns does not correlate well with the seismic damage. Figure 1 shows the degradation of axial load-carrying capacities of the four specimens tested in this experimental study. In the testing, the specimen was loaded until a ductility level of 1.5 suffered minor cracking, which falls into the “slight” damage state based on damage state definitions provided in Table 1 and Table 2. The specimen was loaded until a ductility level of 3.0 suffered wider horizontal and vertical cracks and spalling of concrete at the bottom of the column, which falls into the “moderate” damage state. The specimen was loaded until a ductility level of 4.5 had extensive yielding of steel and spalling of concrete in the core region at the bottom of the column, therefore falling into the “extensive” damage state. The results presented in Figure 1 suggest that even bridge columns with extensive lateral damage are able to carry axial traffic loads up to approximately 80% of the original axial load capacity. From the results of this experimental study, it is seen that bridge columns designed following modern design requirements might maintain a significant amount of their axial load capacity even with the presence of moderate to extensive damage.

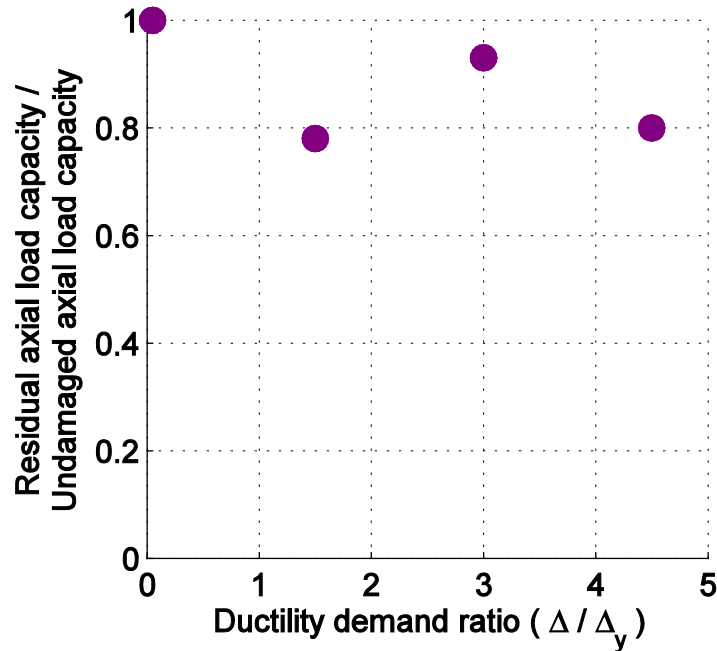


Figure 1. Degradation of axial load-carrying capacity of laterally damaged columns (Terzic and Stojadinovic 2010)

6 Finite element modeling

The residual axial capacity of a reinforced concrete bridge column can be determined through numerical analysis performed on the detailed finite element models of the columns. A finite element model of the prototype reinforced concrete bridge columns was developed and numerical earthquake simulations were performed in this study to obtain the axial capacity of columns. The results of the numerical simulations were compared to the experimental results (Terzic and Stojadinovic 2010) to demonstrate the computational difficulty of finite element modeling in calculating the residual capacity and therefore the need for a simple model that can be used to rapidly estimate the residual load capacity of bridge columns following earthquakes. The finite element model is developed using OpenSees (McKenna 1997), which is a finite element software for simulating the seismic response of structural systems.

The finite element modeling details of bridge columns are shown in Figure 2. The finite element model was developed for a prototype column of a single-column-bent overpass bridge as illustrated in Figure 2a. The column was modeled using force-based fiber elements in OpenSees and the bridge slab and the deck are modeled using rigid elements, as shown in Figure 2b. The

fiber elements are connected to each other through five integration points. The fiber configuration of a cross-section is presented in Figure 2c. In this configuration, the core region of the section consists of 24 fibers, and the cover region consists of 88 fibers. Each reinforcing bar is represented by a single fiber. The concrete and reinforcing steel bar were modeled using the available material stress-strain relationships in Opensees. For this study, the Concrete02 material model was used to model the concrete and the ReinforcingSteel material model was used to model the reinforcing bars. The material properties for the confined region of the concrete were calculated using the material model proposed by Mander et al. (1988).

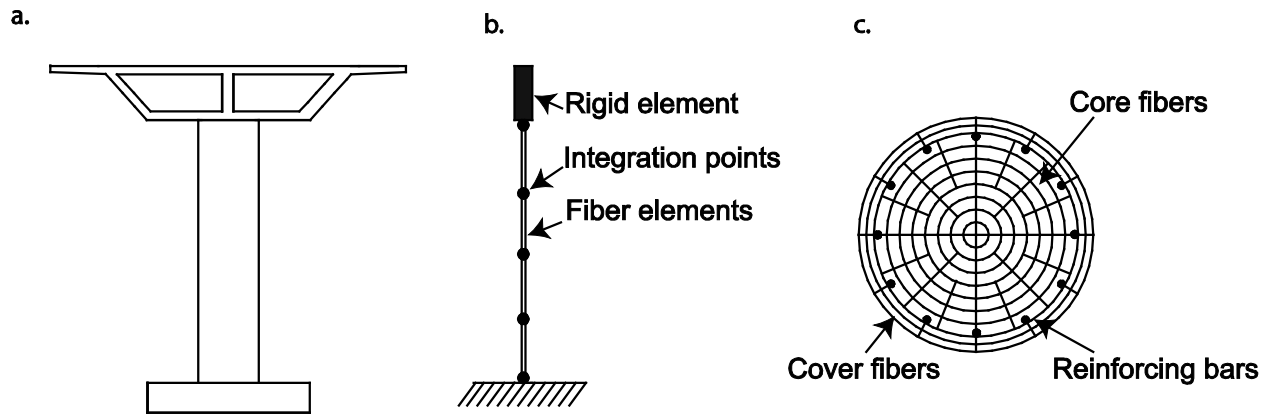


Figure 2. Finite element modeling details: (a) prototype bridge column; (b) fiber-element model of the column; (c) fiber configuration of a cross section

The finite element model of the bridge columns investigated in this study was validated using the experimental study on circular bridge columns performed by Terzic and Stojadinovic (2010). In this experimental study, three cantilever column specimens were first subjected to bilateral cyclic loading up to a pre-determined level of displacement ductility and then axially loaded until the specimens failed. During the lateral loading, a constant 100 kips of axial load, which is approximately 10% of the nominal capacity of the specimens, was maintained to consider the dead and live loads. One additional specimen was only loaded axially in order to obtain the axial capacity of an undamaged reinforced concrete column. The geometric properties and reinforcement details of the specimens tested in this experimental study are presented in Figure 3. The column specimens had an effective height of 64 inches and a diameter of 16 inches. The

cross-section consisted of 12 No. 4 reinforcing bars and W3.5 continuous spiral steel transverse reinforcement, which was located from inside of the column with a clear cover of 0.5 inch.

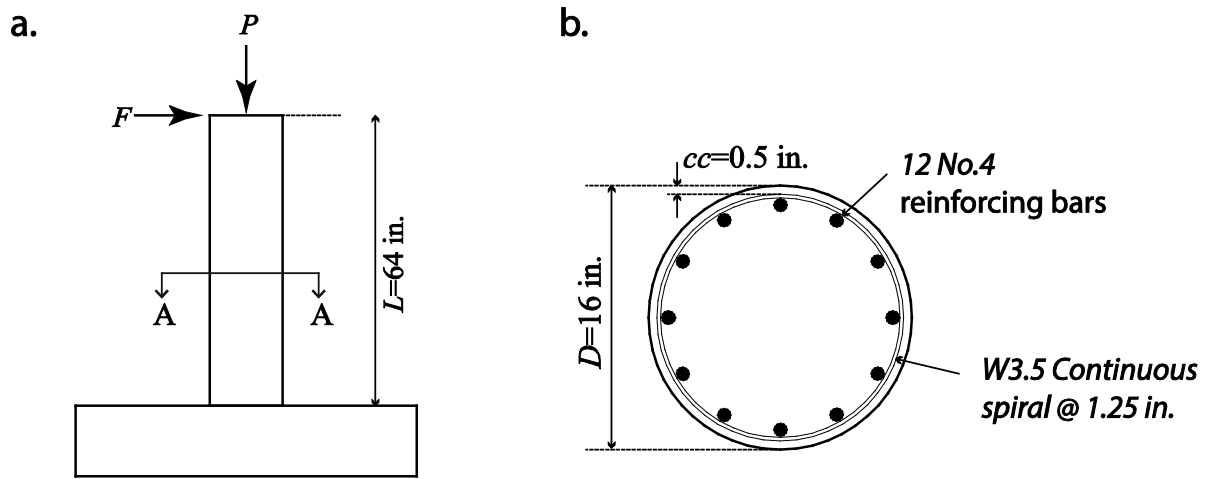


Figure 3. Geometry and reinforcement details of specimens (Terzic and Stojadinovic, 2010): (a) elevation profile; (b) cross section (A-A)

The material properties for concrete and reinforcing steel bars are provided in Table 3.

Table 3. Material properties of specimens

Property Unit	Specimen				
	Base 0	Base 15	Base 30	Base 45	
<i>Concrete</i>					
Concrete compressive strength at 28 days, f_c	ksi	5.48	5.05	4.96	5.09
Concrete strain at maximum strength, ϵ_{c0}	-	0.003	0.003	0.003	0.003
Concrete crushing strength, f_{cu}	ksi	3.79	3.76	3.72	3.76
Concrete strain at crushing strength, ϵ_{cu}	-	0.022	0.024	0.024	0.024
<i>Reinforcing steel bars</i>					
Yield strength of reinforcing bars, f_y	ksi	70.7	70.7	70.7	70.7
Initial modulus of elasticity, E_s	ksi	29000	29000	29000	29000
Ultimate strength of reinforcing bars, f_u	ksi	120	120	120	120
Strain at initial strain hardening, ϵ_{sh}	-	0.01	0.01	0.01	0.01
Strain at peak stress	-	0.12	0.12	0.12	0.12

The numerical earthquake simulations of finite element models were performed with the same bilateral loading history used in experimental testing ((Terzic and Stojadinovic, 2010). The comparison of lateral force-displacement response of the specimen Base 45 to the results of the numerical simulations of finite element model of the same specimen is presented in Figure 4. The results show that the model is capable of predicting the lateral response of bridge columns in both major directions, X and Y, with reasonable accuracy.

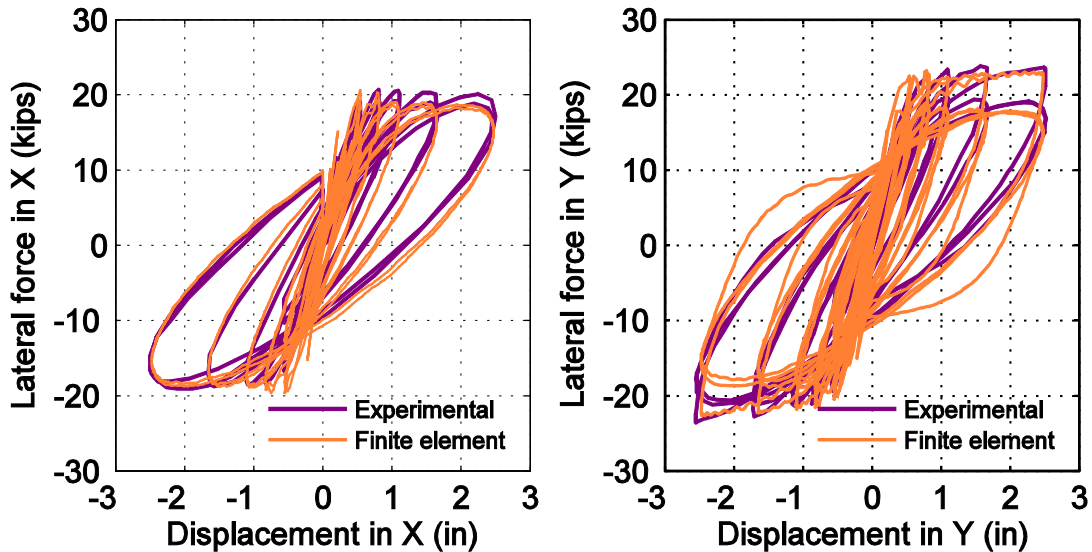


Figure 4. Lateral force-displacement response for specimen Base 45: (a) in X direction; (b) in Y direction

Following the lateral loading phase in the numerical simulation, the analytical models were loaded with an incremental axial load until the specimens failed, as it was performed in the experimental testing. This axial loading phase, which is called pushdown analysis, facilitates the generation of axial force axial displacement relationships for finite element models of column specimens. Figure 5 presents the comparison of the results of the pushdown analysis to the experimental results for four specimens modeled in this study. The maximum axial force observed in the axial force-axial displacement results is the residual axial capacity of the specimen. The results show that the numerical simulation of the finite element models of bridge columns is able to predict the residual axial capacity of the bridge column with reasonable accuracy (i.e., less than 10% error). The error of residual axial capacity in specimen Base 15 (Figure 5b) is slightly higher than those of other specimens, which is mainly due to the residual

drift observed before the axial loading phase in specimen Base 15, while no residual load is observed before the axial loading phase in other specimens and the finite element model was not able to successfully simulate the effects of residual drifts.

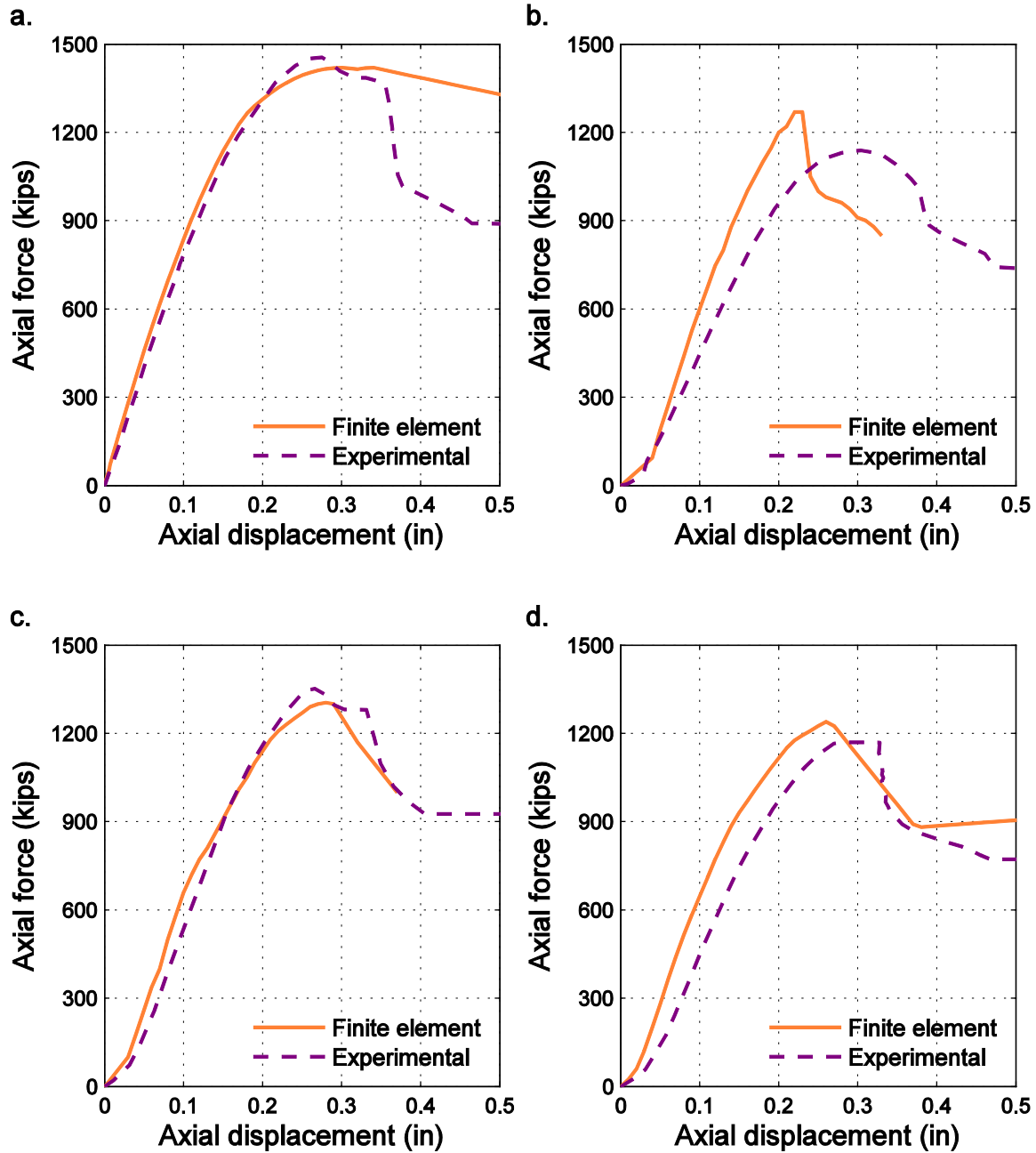


Figure 5. Axial force-displacement relationship for finite element modeling and experimental results for specimens: (a) Base 0; (b) Base 15; (c) Base 30; (d) Base 45

7 Practical method

A practical mechanics-based method is proposed for estimating the residual axial load capacity of damaged reinforced concrete bridge columns. The flowchart of this method is presented in Figure 6. Based on this method, the two input demand parameters are utilized by several mechanics-based models. These input demand parameters are: (1) the maximum displacement at the column top observed during the earthquake ground shaking, and (2) the residual displacement at the column top at the end of the earthquake ground shaking. In the mechanics-based model, the residual axial load capacity of concrete and reinforcing bars in a column section are calculated and are summed to obtain the residual axial capacity of the column, same as the axial capacity calculation of undamaged columns. The residual axial capacity of a column section, P_r , is therefore calculated according to:

$$P_r = P_c + P_s \quad (1)$$

where P_c is the residual axial load capacity of the concrete, and P_s is the residual axial load capacity of the reinforcing steel bars. Each individual task on the flowchart is described in detail in the following subsections. It should be noted that the derivations given in these subsections are made for single circular bridge columns and for bilateral loading; however, similar formulations can also be used for the residual axial load capacity calculations for other cross-section types and different loading patterns.

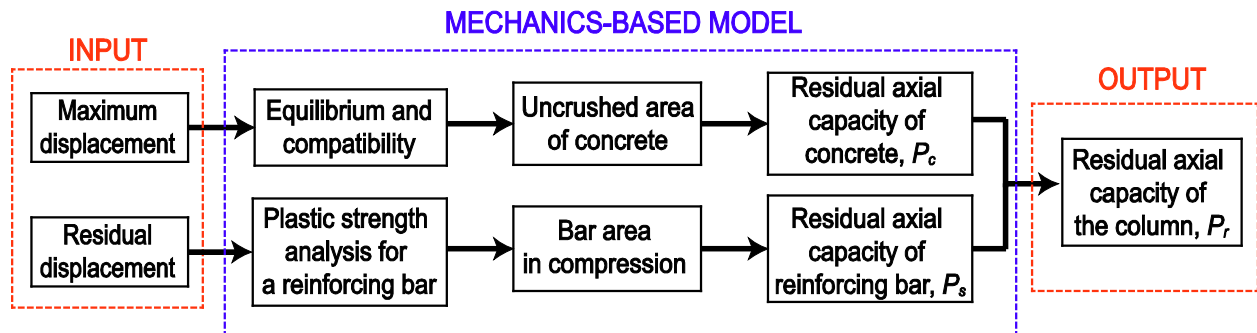


Figure 6. Flowchart of the practical method

7.1 Determination of the uncrushed area of the column

During the lateral loading, compressive strain at the outermost fibers of reinforced concrete sections might exceed the crushing strain value of concrete, and therefore these crushed regions become unable to carry further loads. Therefore, the axial load that can be carried by the column decreases. The uncrushed area of the reinforced concrete section can be calculated using sectional analysis based on force equilibrium at the maximum lateral displacement. Figure 7 presents the stresses and strains of the concrete and reinforcing steel bars at the maximum displacement to calculate the uncrushed area. In this figure, P and M are the axial load and moment on the section at the maximum lateral drift, c is the neutral axis depth, x is the depth of the uncrushed region from the neutral axis, ϵ_{cu} is the crushing strain of the concrete, ϕ_{\max} is the curvature of the section at the maximum displacement, β_1 is the ratio of depth of rectangular block to depth of neutral axis, f_c is the compressive strength of concrete, and f_1 to f_7 represent the stresses at the reinforcing steel bars located at the same level. The depth of the uncrushed region, x , is calculated through an iterative process using the force and moment equilibrium on the cross section according to:

$$P = \sum_{i=1}^m f_i A_{bar,i} + 0.85 f_c A_c \quad (2)$$

$$M = \sum_{i=1}^m f_i A_{bar,i} \bar{y}_i + 0.85 f_c A_c \bar{y}_c \quad (3)$$

where m is the number of reinforcing steel bar layers in the column section, $A_{s,i}$ is the sum of the area of reinforcing bars at the i th level of the cross-section, A_c is the area of the compression zone of the equivalent concrete stress block, \bar{y}_i is the distance from a reinforcing bar level to the centroid of the gross section, and \bar{y}_c is the distance from the centroid of the compression zone area of the equivalent concrete stress block to the centroid of the gross section.

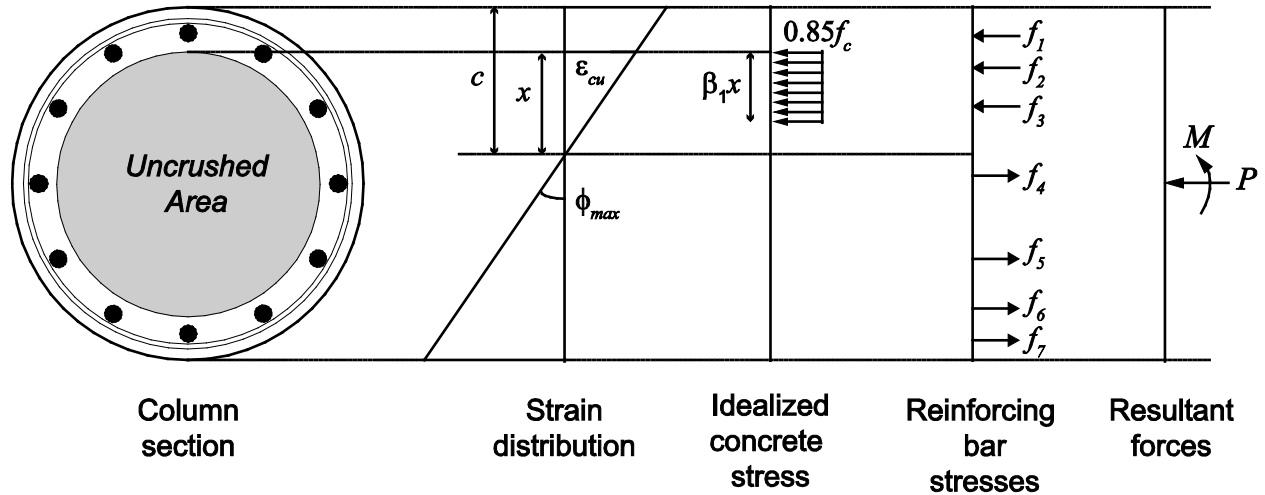


Figure 7. Equilibrium and compatibility diagram at the maximum displacement

The maximum curvature, which is used to find the strain configuration, is calculated based on the inelastic deformation of bridge columns, as illustrated in Figure 8. Based on the inelastic deformation of bridge columns, the curvature at the maximum drift, ϕ_{max} , is the sum of the yield curvature, ϕ_y and the plastic curvature, ϕ_p , as follows:

$$\phi_{max} = \phi_y + \phi_p \quad (4)$$

The yield curvature in Equation 4 can be computed according to Priestley et al. (1996):

$$\phi_y = \frac{\lambda \epsilon_y}{D} \quad (5)$$

where λ is taken as 2.45 for spiral columns (Berry and Eberhard 2004), ϵ_y is the yield strain of reinforcing steel bar, and D is the diameter of column. The plastic curvature, ϕ_p , in Equation 4 is calculated according to:

$$\phi_p = \frac{\theta_p}{L_p} \quad (6)$$

where L_p is the plastic hinge length, which can be calculated according to Paulay and Priestley (1992):

$$L_p = 0.08L + 0.15f_y d_b \geq 0.3f_y d_b \quad (7)$$

where L is the length of the column, f_y is the yield strength of reinforcing bars, and d_b is the diameter of reinforcing bars. In Equation 6, θ_p is the plastic rotation of the column calculated using:

$$\theta_p = \frac{\Delta_p}{\left(L - \frac{L_p}{2}\right)} \quad (8)$$

where Δ_p is the plastic displacement. The maximum displacement, Δ_{max} , can be defined as the summation of the yield displacement, Δ_y , and the plastic displacement, Δ_p , based on the deflected shape of the column given in Figure 8. Therefore, Δ_p can be calculated using:

$$\Delta_p = \Delta_{max} - \Delta_y \quad (9)$$

where Δ_y is the yield displacement calculated according to Priestley et al. (1996):

$$\Delta_y = \frac{\phi_y L^2}{3} \quad (10)$$

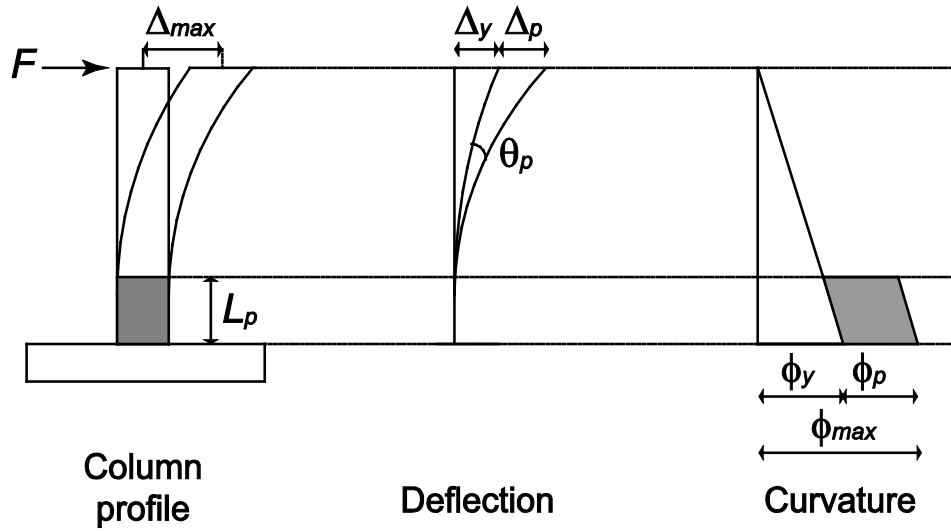


Figure 8. Inelastic deformation of a bridge column (adapted from Priestley et al. 1996)

The moment resulting from the axial load and the lateral displacement is calculated based on the force equilibrium on the column, shown in Figure 9 and using the following equation:

$$M = P\Delta + FL \quad (11)$$

where F is the lateral load at which maximum displacement occurs.

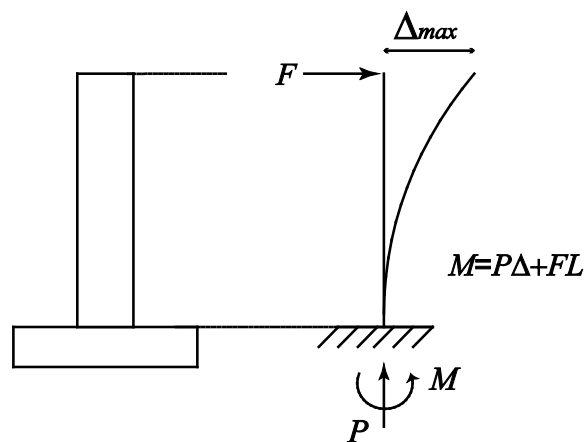


Figure 9. Force equilibrium on the column

The equivalent concrete block stress and the reinforcing bar stresses at the maximum displacement are computed based on stress-strain material models. The material models for concrete and steel used in this study are presented in Figure 10. For the concrete, Mander's (1988) stress-strain model (see Figure 10a) was used, and for reinforcing steel bars a bilinear material model was assumed (see Figure 10b). The Mander stress-strain model computes the compressive strength of the confined concrete, f'_{cc} , according to:

$$f'_{cc} = f'_c \left(2.254 \sqrt{1 + \frac{7.94 f'_l}{f'_c}} - \frac{2 f'_l}{f'_c} - 1.254 \right) \quad (12)$$

where f'_c is the compressive strength of concrete and f'_l is the effective lateral confining stress calculated using:

$$f'_l = k_e f_l \quad (13)$$

$$f_l = 0.5 \rho_s f_{yh} \quad (14)$$

where k_e is a confinement effectiveness coefficient and typically taken as 0.95 for circular sections (Priestley et al. 1996), and ρ_s is the ratio of confining spiral steel bar to the volume of confined concrete, calculated using:

$$\rho_s = \frac{A_{sp} \pi d_s}{\frac{\pi}{4} d_s^2 s} = \frac{4 A_{sp}}{d_s s} \quad (15)$$

where A_{sp} is the area of confining spiral steel bar, d_s is the diameter of spiral bar, and s is the center-to-center spacing of spiral bar.

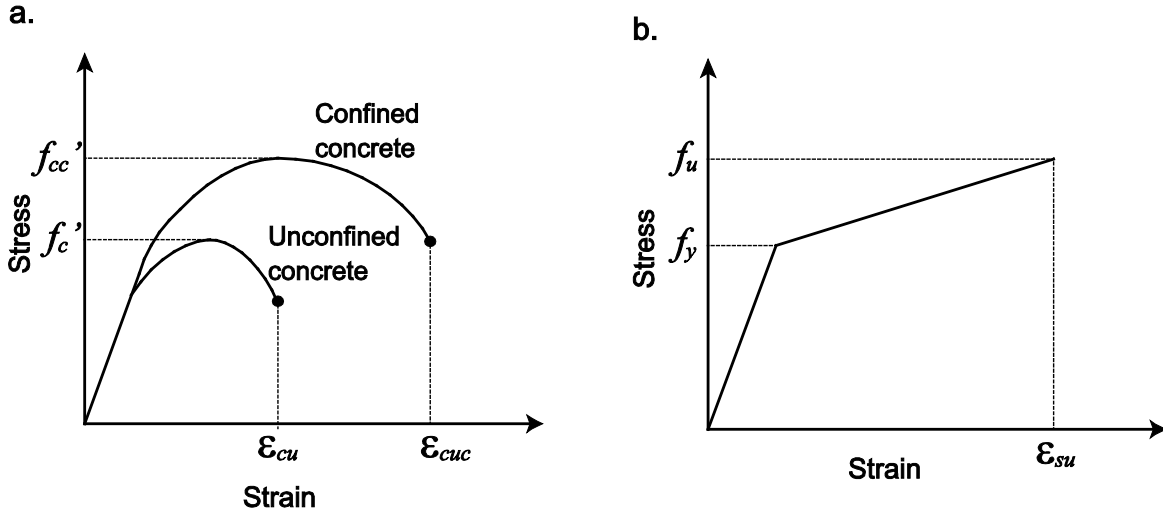


Figure 10. Material models used in the practical method: (a) concrete; (b) reinforcing steel

7.2 Residual axial capacity of concrete region of column

Once the crushing depth of the concrete is determined through sectional analysis, the residual axial load capacity of the concrete part of the column section can be calculated. If the crushing depth remains in the cover region, that is, there is no crushing in the core region, then the full area of the confined concrete region is considered in residual axial load capacity computations because the cover region of the concrete is assumed to spall before the axial failure. In this case, the residual axial load capacity of concrete is calculated according to:

$$P_{c,1} = 0.85 f_{cc} (A_{core} - A_{st}) \quad (16)$$

where A_{core} is the area of the concrete bounded between the spirals and A_{st} is the total area of the reinforcing bars. A_{core} and A_{st} are computed according to:

$$A_{core} = \pi \left(\frac{D}{2} - cc \right)^2 \quad (17)$$

$$A_{st} = n A_{bar} \quad (18)$$

where cc is the clear cover of the column section, n is the number of reinforcing bars, and A_{bar} is the cross-sectional area of a reinforcing bar.

If there is crushing in the core region, then the residual axial load capacity of concrete is calculated by taking the uncrushed area of the concrete core into account according to:

$$P_{c,2} = 0.85 f_{cc} (A_{uncrushed}) \quad (19)$$

where the area of the uncrushed concrete is calculated according to:

$$A_{uncrushed} = \pi \left(\frac{D}{2} - c + x \right)^2 \quad (20)$$

To summarize, the following is proposed for the calculation of the residual axial load capacity of concrete, P_c :

$$\begin{aligned} P_c &= P_{c,1} && \text{when there is no crushing in the core} \\ P_c &= P_{c,2} && \text{when there is crushing in the core} \end{aligned} \quad (21)$$

7.3 Residual axial load capacity of reinforcing steel bars

The longitudinal reinforcing bars are able to carry axial loads up to their buckling or plastic capacities (Elwood and Moehle 2005). The plastic strength of the reinforcing bars in deformed shape is illustrated in Figure 11. The plastic moment capacity of one reinforcing bar of a bridge column, M_p , can be related to its plastic axial capacity, $P_{s,p}$, as follows:

$$M_p = \Delta_r P_{s,p} \quad (22)$$

where Δ_r is the residual displacement of the column at the end of the lateral loading. From the axial force and moment equilibrium on the reinforcing bar section, as illustrated in Figure 11, the following equations can be obtained:

$$M_p = 2A_{tens}f_y y_{tens} \quad (23)$$

$$P_{s,p} = (A_{bar} - 2A_{tens})f_y \quad (24)$$

where A_{tens} is the area of the reinforcing bar in tension, and y_{tens} is the distance from the centroid of the reinforcing bar to the centroid of the tension area. From Equations 23 and 24, the plastic axial capacity of a bar can be calculated by iteratively changing the A_{tens} value. The buckling capacity of the reinforcing bar is calculated according to Elwood and Moehle (2005):

$$P_{s,b} = \frac{0.1\pi^2 E_s I_{bar}}{S^2}$$

The total residual axial load capacity of the reinforcing steel bars is then calculated according to:

$$P_s = nP_{s,p} < nP_{s,b} \quad (25)$$

Calculation of the residual axial load capacity of concrete, P_c , and the residual axial load capacity of reinforcing steel bars, P_s , facilitates the calculation of the residual axial load capacity of the column section, P_r , based on Equation 1.

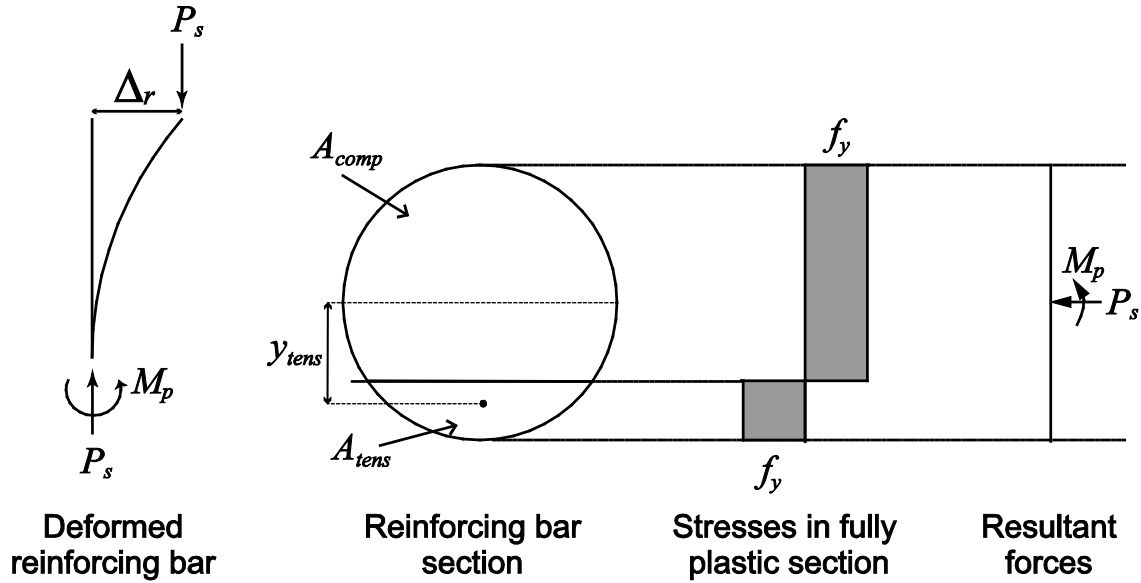


Figure 11. Plastic strength of a reinforcing bar

8 Validation of the model

The proposed mechanistic model in this study has been validated using the experimental study on circular bridge columns performed by Terzic and Stojadinovic (2010). As stated previously, this experimental study has two loading phases. In the first phase, the specimens are displaced up to a pre-determined level of displacement ductility by bilateral, quasi-static circular loading. In the second phase, damaged columns are re-centered and axially compressed until they fail. The simulation details and the observed damage in this testing sequence are summarized in Table 4. Although all specimens are re-centered following the lateral loading and before the application of the axial test, a 1% residual drift is observed in the specimen Base15. The axial capacities determined at the end of the testing are also presented in the last row of Table 4.

Table 4. Lateral loading information, observed damage and residual axial load capacity of specimens

<i>Loading or damage information</i>	<i>Specimen</i>			
	<i>Base 0</i>	<i>Base 15</i>	<i>Base 30</i>	<i>Base 45</i>
Displacement ductility level	No lateral loading	1.5	3.0	4.5
Damage during the lateral loading	N.A	No visible cracks	Horizontal cracks, vertical cracks less than 1/32 inch, and some spalling of concrete at the bottom 8 in. of the column	Extensive yielding of steel and spalling of concrete, reduction in volume of concrete core in the plastic hinge region
Residual drift at the end of the lateral loading	No	1 %	No	No
Axial capacity following lateral loading (kips)	1459	1137	1355	1170

The input parameters used in the mechanistic model are provided in Table 5. As the geometric properties of specimens are shown in Figure 3, these parameters are not included in Table 5.

Table 5. The input parameters for the mechanistic model

<i>Property</i>	<i>Unit</i>	<i>Specimen</i>			
		<i>Base 0</i>	<i>Base 15</i>	<i>Base 30</i>	<i>Base 45</i>
Maximum displacement, Δ_{max}	in.	0	0.83	1.67	2.45
Residual displacement, Δ_r	in.	0	0.64	0	0
Lateral force at peak displacement, F	kips	0	18	20	22
Unconfined compressive strength, f_c	ksi	5.48	5.05	4.96	5.09
Yield strength of reinforcing bars, f_y	ksi	70.7	70.7	70.7	70.7
Ultimate strength of reinforcing bars, f_u	ksi	120	120	120	120
Yield strength of spirals, f_{yh}	ksi	95	95	95	95

The residual axial load capacities of each specimen calculated using the proposed model are compared to the experimental results in Figure 12. The relative error between the axial capacity estimated by the model and the experimental capacity for each specimen is presented in Figure 13. From Figures 12 and 13, the relative error is seen to be less than 3% in all specimens. This demonstrates that the proposed model is able to accurately estimate the residual axial load capacities of flexure-dominated circular bridge columns. From this validation study, it is shown that the proposed model requires less effort to estimate the residual axial load capacity than detailed finite element modeling requires. Therefore, this model can be used as a rapid post-event assessment tool regarding the functionality of bridges.

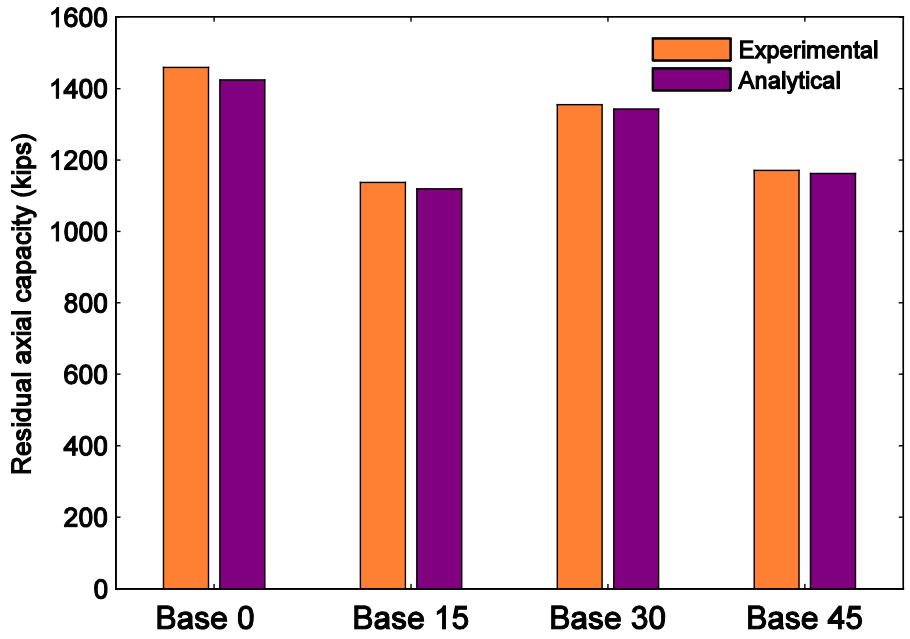


Figure 12. Comparison of residual axial load capacity estimation to experimental results

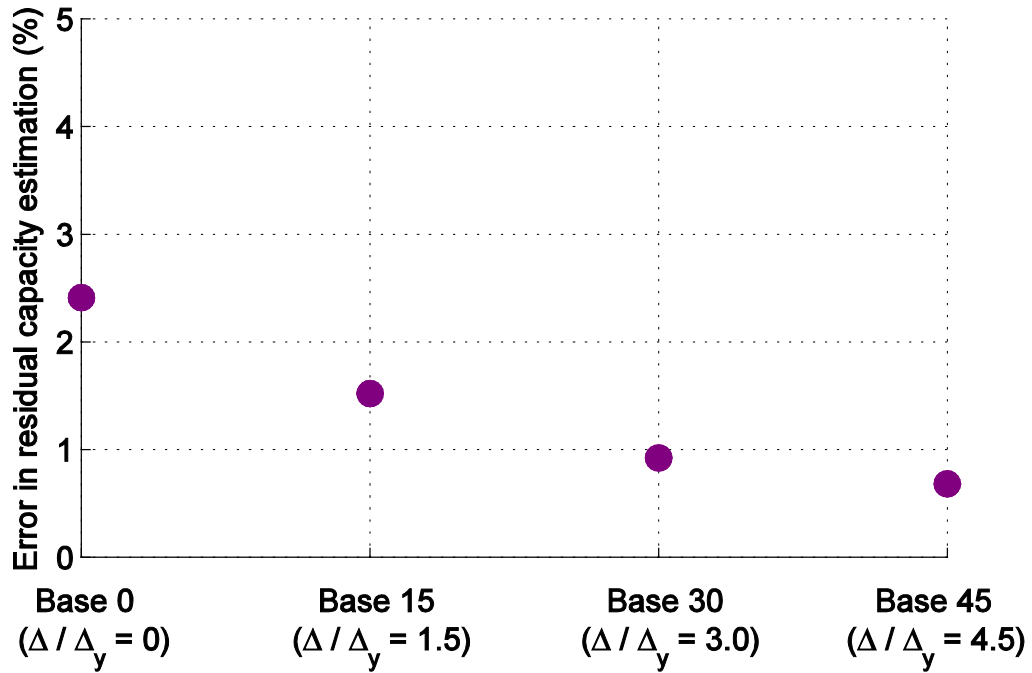


Figure 13. Relative error in residual axial capacity estimation for each specimen

9 Sensitivity analysis

Sensitivity analysis is performed to identify parameters to which the model's output is most sensitive. The results of the sensitivity analysis facilitate an understanding of the relative importance of input parameters on the residual axial load capacity. This understanding can guide the refinement of the model by removing the parameters to which the residual axial capacity is insensitive. In this study, the Sobol method (Sobol 1993, 2001) is used for sensitivity analysis. The Sobol method is a global sensitivity analysis technique, in that it examines an integrated sensitivity over the entire input parameter space. The Sobol method is a variance-based method where the contribution of each input parameter to the total variance of the output is quantified by decomposing the variance of the model's output into variance of model parameters according to:

$$V(y) = \sum_i V_i + \sum_i \sum_{j>1} V_{ij} + \dots + V_{12\dots k} \quad (26)$$

where V_i is the first-order model output variance due to the i th component of a given input parameter x_i and V_{ij} is the second-order model output variance due to the interaction between i th and j th component of given input parameters x_i and x_j . The sensitivity of the output $V(y)$ to variation of the input parameters, x_1 to x_n , is quantified using a first-order sensitivity index, S_i , by using:

$$S_i = \frac{V_i}{V(y)} \quad (27)$$

A total order sensitivity index, S_{Ti} , is also used to measure the sensitivity of the output to a parameter plus its interactions with other parameters calculated according to:

$$S_{Ti} = 1 - \frac{V_{\sim i}}{V(y)} \quad (28)$$

where $V_{\sim i}$ is the average variance of all parameters except x_i .

The Sobol method is used to compute the sensitivity indices for the key parameters of the residual axial load capacity estimation model proposed in this study. Nine independent input parameters are identified in the model and listed in Table 6. A uniform distribution is assumed for each parameter, with the range of parameters being within $\pm 5\%$ of the nominal value.

Table 6. Parameters and parameter ranges considered in the sensitivity analysis

Number	Parameter Name	Symbol	Unit	Range
1	Concrete compressive strength	f_c	ksi	4.8-5.2
2	Yield strength of reinforcing steel bars	f_y	ksi	65-75
3	Ultimate strength of reinforcing steel bars	f_u	ksi	110-130
4	Yield strength of spirals	f_{yh}	ksi	95-105
5	Column length	L	in.	62-66
6	Column diameter	D	in.	15.5-16.5
7	Reinforcing bar diameter	d_b	in.	0.45-0.55
8	Spiral diameter	d_{sp}	in.	0.2-0.22
9	Spiral spacing	s	in.	1.2-1.3

The sensitivity analyses are performed for each specimen of Terzic and Stojadinovic (2010), which are used to validate the model. The first-order and total-order sensitivity indices obtained from the sensitivity analysis are presented in Figure 14 for each specimen. From sensitivity indices for the specimen Base 0, which is presented in Figure 14a, the residual axial load capacity is found to be most sensitive to compressive strength of concrete, f_c , and the column diameter, D . The yield strength of steel, f_y , and the length of the column, L , on the other hand, have negligible effects on the residual axial load capacity. Similar findings are obtained for the specimens Base 15 and Base 30, which are presented in Figure 14b and Figure 14c. However, as the target displacement ductility of the loading increases, the residual axial load capacity becomes more sensitive to the diameter of the column. These results are expected because the residual capacity estimations are mostly based on the cross-sectional area of the columns, which is a function of the column diameter. The sensitivity indices for specimen Base 45, which are presented in Figure 14d, show different trends than other specimens. In this case, the residual axial load capacity is found to be sensitive to spiral diameter, d_{sp} , reinforcing bar diameter, d_b ,

and length, L , of the column in addition to compressive strength of concrete, f_c , and the column diameter, D . The main reason for the change in the sensitivity trends in the specimen Base 45 is that the crushing occurs in the core region of the column at higher displacement ductility levels and therefore the inelastic deformation of columns is taken into account (See Figure 8). The sensitivity indices presented in Figure 13 suggests that the further simplification on the parameters of the model might not be possible because all parameters become relatively important when crushing occurs on the core region at higher displacements.

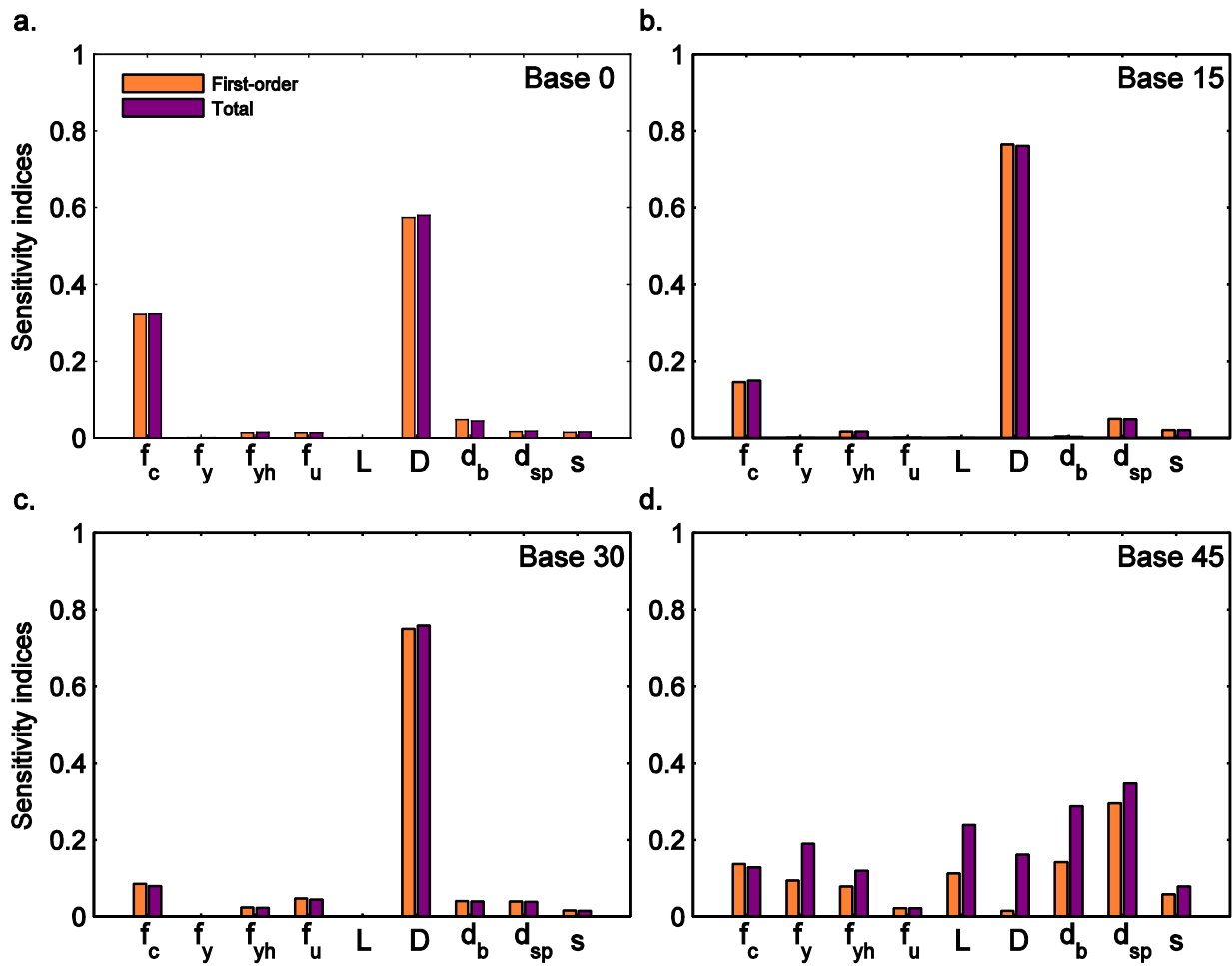


Figure 14. Sensitivity indices for each specimen

10 Summary and conclusions

A practical method to estimate the residual axial load capacity of reinforced concrete bridge columns, given a demand, has been developed. The method is based on mechanics and utilizes plastic hinge development of columns and cross-sectional analysis. The method is based on the notion that the residual axial load capacity of a column is the sum of the remaining axial capacities of concrete and reinforcing steel bars. More specifically, the concrete and reinforcing bars share the axial load capacity based on the multiplication of their strengths with their deformed cross-sectional areas. For the axial capacity calculation of a damaged column, the uncrushed concrete area, rather than the gross area, is considered, where the crushing depth of the concrete is computed using the stress-strain distributions of concrete and reinforcing steel bars at the maximum drift. The residual axial load capacity of reinforcing bars is determined through plastic strength analysis of the bars using the residual displacement at the end of the lateral loading. The developed model is validated using the results of past experimental testing on column specimens. Based on the results and findings of this study, the following conclusions are provided:

- (1) The practical method is computationally efficient yet offers high fidelity in that it was shown to be capable of estimating the residual axial load capacity of bridge columns with a reasonable accuracy (i.e., less than 3% relative error) when compared to past experimental results for columns dominated by flexure and designed according to modern standards.
- (2) The model is parsimonious in that the results of the sensitivity analysis suggest no further simplification (i.e., elimination of parameters) is possible since as demand increases, the residual axial load capacity becomes sensitive to the variations in all the input parameters (see Figure 14).
- (3) This study explores the mechanistic relationship between lateral seismic demand and the residual load capacity of a flexure-dominated single bridge column. This relationship can be used to simulate the impact of regional hazards on the functionality of transportation networks for disaster planning and loss estimation.

11 References

- [1] Basoz, N., and Mander, J. (1999). *Enhancement of the Highway Transportation Lifeline Module in HAZUS*, National Institute of Building Sciences.
- [2] Berry, M., and Eberhard, M. O. (2004). *Performance Models for Flexural Damage in Reinforced Concrete Columns*. Pacific Earthquake Engineering Research Center, PEER 2007/07, Berkeley, CA.
- [3] Caltrans. (2006). "Seismic Design Criteria." State of California Department of Transportation.
- [4] Choi, E., DesRoches, R., and Nielson, B. (2004). "Seismic Fragility of Typical Bridges in Moderate Seismic Zones." *Engineering Structures*, 26(2), 187-199.
- [5] Elwood, K. J., and Moehle, J. P. (2005). "Axial capacity model for shear-damaged columns." *ACI Structural Journal*, 102(4).
- [6] Elwood, K. J. (2004). "Modelling failures in existing reinforced concrete columns." *Canadian Journal of Civil Engineering*, 31(5), 846-859.
- [7] FEMA (2003). *HAZUS-MH MRI: Technical Manual, Vol. Earthquake Model*. Federal Emergency Management Agency, Washington DC.
- [8] Hachem, M. M., Moehle, J. P., and Mahin, S. A. (2003). "Performance of circular reinforced concrete bridge columns under bidirectional earthquake loading," PEER 2003/06, Pacific Earthquake Engineering Research Center.
- [9] Henry, L., and Mahin, S. A. (1999). *Study of buckling of longitudinal bars in reinforced concrete bridge columns*. California Dept. of Transportation.
- [10] Indiana Department of Transportation (INDOT) (2000). *Handbook for the Post-Earthquake Safety Evaluation of Bridges and Roads*, JTRP Contract No. 2377.
- [11] Kunnath, S., El-Bahy, A., Taylor, A., and Stone, W. (1997). *Cumulative seismic damage of reinforced concrete bridge piers*, National Center for Earthquake Engineering Research, NCEER-97-0006, Buffalo, N.Y.
- [12] Lehman, D. E., and Moehle, J. P. (2000). *Seismic Performance of Well-Confined Concrete Bridge Columns*, Pacific Earthquake Engineering Research Center, PEER 1998/01, Berkeley, CA.
- [13] Mckenna, F. T., Fenves, G. L., Scott, M. H., and Jeremi, B. (2000). "Open System for Earthquake Engineering Simulation". <<http://OpenSEES.berkeley.edu>>.

- [14] Mackie, K. R., and Stojadinović, B. (2005). *Fragility basis for California highway overpass bridge seismic decision making*. Pacific Earthquake Engineering Research Center, PEER 2005/12, Berkeley, CA.
- [15] Mander, J. B., Priestley, M. J., and Park, R. (1988). “Theoretical stress-strain model for confined concrete.” *Journal of Structural Engineering*, 114(8), 1804-1826.
- [16] Moyer, M., and Kowalsky, M. (2001). “Influence of tension strain on buckling of reinforcement in rc bridge columns.” Master’s thesis, North Carolina State University.
- [17] Munro, I., Park, R., and Priestley, M. (1976). *Seismic behavior of reinforced concrete bridge piers*. Department of Civil Engineering, Report 76-9, University of Canterbury, Christchurch, New Zealand.
- [18] Paulay, T., and Priestley, M. N. (1992). *Seismic design of reinforced concrete and masonry buildings*. Wiley, New York.
- [19] Priestley, M. N. (1996). *Seismic design and retrofit of bridges*. John Wiley & Sons, New York.
- [20] Sobol’, I. M. (1993). “Sensitivity analysis for non-linear mathematical models.” *Mathematical Modeling and Computational Experiments*, 1(4), 407–414.
- [21] Sobol’, I. M. (2001). “Global sensitivity indices for nonlinear mathematical models and their Monte Carlo estimates.” *Mathematical and Computational Simulation*, 55(1–3), 271–280.
- [22] Tasai, A. (2000). *Residual axial capacity of reinforced concrete columns during shear degradation*. Pacific Earthquake Engineering Research Center, PEER 10, Berkeley, CA, 257-267.
- [23] Tasai, A. (1999). “Residual axial capacity and restorability of reinforced concrete columns damaged due to earthquake.” In US-Japan Workshop on Performance-Based Earthquake Engineering Methodology for Reinforced Concrete Building Structures (pp. 191-202).
- [24] Terzic, V., and Stojadinovic, B. (2010). *Post-Earthquake Traffic Capacity of Modern Bridges in California*, Pacific Earthquake Engineering Research Center, PEER 2010/103, Berkeley, CA.